

# Differential Contrastive Training for Gaze Estimation

Lin Zhang, Yi Tian\*, XiYun Wang, Wanru Xu, Yi Jin, Yaping Huang  
Beijing Jiaotong University

## Abstract

The complex application scenarios have raised critical requirements for precise and generalizable gaze estimation methods. Recently, the pre-trained CLIP has achieved remarkable performance on various vision tasks, but its potentials have not been fully exploited in gaze estimation. In this paper, we propose a novel Differential Contrastive Training strategy, which boosts gaze estimation performance with the help of the CLIP. Accordingly, a Differential Contrastive Gaze Estimation network (DCGaze) composed of a Visual Appearance-aware branch and a Semantic Difference-aware branch is introduced. The Visual Appearance-aware branch is essentially a primary gaze estimation network and it incorporates an Adaptive Feature-refinement Unit (AFU) and a Double-head Gaze Regressor (DGR), which both help the primary network to extract informative and gaze-related appearance features. Moreover, the Semantic Difference-aware branch is designed on the basis of the CLIP’s text encoder to reveal the semantic difference of gazes. This branch could further empower the Visual Appearance-aware branch with the capability of characterizing the gaze-related semantic information. Extensive experimental results on four challenging datasets over within and cross-domain tasks demonstrate the effectiveness of our DCGaze. Code will be available upon acceptance.

## 1. Introduction

Gaze estimation aims to predict a 2D gaze position or a 3D gaze direction of a specified user given its facial or eye image. As an important task in the field of computer vision, it has been extensively utilized in various people-related researches, such as virtual reality [4, 23], autonomous driving [11, 28], etc. In those real scenarios, the users identities and their surrounding environments are changeable and complicated, which puts a heavy responsibility on the accuracy and generalization of gaze estimation models. In other words, the estimation models that are optimized via training users should adapt to disjointed new subjects accurately.

Most recently, the pre-trained Visual-Language models

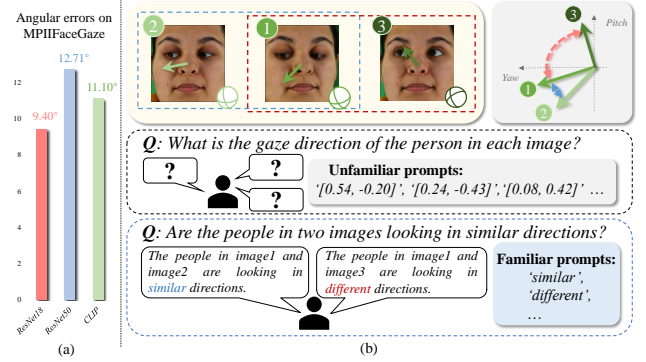


Figure 1. (a) The gaze errors of ResNet18, ResNet50 and CLIP on MPIIFaceGaze dataset. We evaluate ResNet18 and ResNet50 on the cross-domain task  $\mathcal{D}_E \rightarrow \mathcal{D}_M$ , which indicates training on ETH-XGaze and testing on MPIIFaceGaze. (b) Comparing with generating a unique sentence for each image, it is more easier to describe the gaze differences of a pair of images.

represented by CLIP [31] have demonstrated impressive performance on various perception tasks, like image classification [12], semantic segmentation [55], depth estimation [46, 47] and others [17]. CLIP trains an image encoder and a text encoder jointly by a contrastive loss in the embedding space between both modalities, which endows it with powerful representation capabilities by characterizing both visual and semantic information of a target object. Naturally, we are spontaneously curious about the issue: **can CLIP understand human gaze?** To explore this concern, we make a simple early attempt. Inspired by [47], we define four gaze bins that align with the gaze directions of  $[0, \frac{\pi}{2}]$ ,  $[0, -\frac{\pi}{2}]$ ,  $[\frac{\pi}{2}, 0]$  and  $[-\frac{\pi}{2}, 0]$ , respectively. And their semantic descriptions are designated as a prescribed prompt 'A photo of a face gazing {gaze direction}', where gaze direction includes ['up', 'down', 'left', 'right']. Then the gaze direction of an arbitrary facial image could be obtained via linearly combining the multi-bin gaze values according to the language-image similarities between its visual embedding and semantic embeddings of all the gaze bins (details refer to supplementary materials). Surprisingly, even without fine-tuning on any exclusive gaze estimation datasets, the CLIP achieves promising performance comparable to ResNet18 and ResNet50 that trained with cross-domain

samples (Figure 1). From the results, we thus draw a rough conclusion that *the CLIP could perceive human gazes subtly, but its potentials have not been fully exploited*.

We theoretically analyze the possible reasons hindering the CLIP from reaching its full potentials in perceiving gaze directions. On the one hand, CLIP has never seen standard ‘face (image)-gaze (text) pairs in its pre-training stage. This makes it difficult for CLIP to understand the meaning of gaze directions, e.g., [0.54 (pitch), -0.20 (yaw)]. On the other hand, unlike the finite and discrete outputs in typical classification and segmentation tasks, gaze labels are distributed in an infinite and continuous space. Thus, it is difficult to design a set of gaze-guided text prompts that can fittingly align with each facial image. In other words, the challenges in connecting text prompts with gaze labels obstruct the extraction of gaze-related semantic information.

Recently, several studies [38, 45] have attempted to take advantage of CLIP to predict gaze directions. The notable CLIP-Gaze [45] aims to purify gaze-relevant features by pushing away the extracted gaze features from gaze-irrelevant semantic embeddings obtained via the text encoder of CLIP. Essentially, it employs the text encoder to generate gaze distractors rather than describe the gaze itself, which remains unable to solve the above issues.

To address the aforementioned challenges, in this paper, we put forward an innovative and straightforward **Differential Contrastive Training (DCTrain)** strategy to fully evoke CLIPs potentials in gaze estimation. Commonly, although it is impractical to describe the continuous gaze direction of each facial image in language, it is easier to semantically distinguish the gaze difference between a sample pair. For example, as shown in Figure 1, there are three facial images with gaze directions of [0.54, -0.20], [0.24, -0.43], [0.08, 0.42], respectively. Obviously, we could not generate a unique sentence for each image to explain their detailed gaze directions. While we could clearly draw the conclusions that ‘the people in *image1* and *image2* are looking in much *similar* directions’ and ‘the people in *image1* and *image3* are looking in much *different* directions. Motivated by the common observations, instead of identifying gaze direction of single facial image, our Differential Contrastive Training strategy is designed to leverage CLIP for unveiling gaze semantic differences of image-pairs. Innovatively, this strategy could simplify the target texts that the CLIP needs to understand by replacing its unfamiliar phrases, e.g., ‘[0.54, -0.20]’ with familiar ones, e.g., ‘similar’ or ‘different’ (Figure 1). Moreover, the continuous gaze labels are transformed into discrete similarity levels of a pair of gazes. Thus, the above two challenges are expected to be resolved under our Differential Contrastive Training strategy.

Accordingly, a **Differential Contrastive Gaze Estimation network (DCGaze)** is proposed, which consists

of a Visual Appearance-aware branch and a Semantic Difference-aware branch.

The Visual Appearance-aware branch is essentially a primary gaze estimation network, which extracts the appearance feature of each facial image and then regresses it into a final gaze direction. We employ the remarkable CNN-Transformer architecture as the basic structure of this branch. To ensure that the extracted appearance features are informative and gaze-related, we propose an Adaptive Feature-refinement Unit (AFU) and a Double-head Gaze Regressor (DGR). The former is based on the image encoder of the pre-trained CLIP, which aims to dynamically enhance the gaze-related contents contained in extracted appearance features via thoroughly exploring its relationships with the prior appearance features of CLIP. The Double-head Gaze Regressor is introduced to mitigate the overfitting issues caused by the conventional MLP-based regressor. It incorporates an extra regressor head with random masking policy to prevent itself from excessively focusing on several feature dimensions.

The Semantic Difference-aware branch is built upon the text encoder of CLIP, which could be plug and play to arbitrary gaze estimation models. Firstly, a series of differential gaze prompts are designed, which reveal the relationships of gaze directions between two facial images in language (Table 1). And then, the connections between the semantic embeddings of these prompts and the appearance features of image-pairs captured via the Visual Appearance-aware branch could be established to realize an ‘image-language contrastive learning. To be specific, the ‘image refers to the concatenated appearance features of selected image-pairs. The ‘language refers to the sentence that describes their similarity in terms of true gaze directions. Therefore, by semantically identifying the gaze difference of sample pairs with the help of the Differential Contrastive Training, we can fully leverage the semantic representation ability of CLIP to facilitate the primary gaze estimation model to characterize semantic gaze-related information.

The main contributions of our paper are as follows:

- We develop the potentials of CLIP in boosting gaze estimation performance with a novel **Differential Contrastive Training** strategy. Innovatively, we propose to establish the connections between languages and gaze differences of image -pairs, which could provide new ideas for analogous quantified/regression tasks.
- We propose a novel **Differential Contrastive Gaze Estimation network**, which consists of a Visual Appearance-aware branch and a Semantic Difference-aware branch. The former is designed to extract more robust appearance features and build a generalized regressor. The latter improves the ability to characterize the semantic gaze-related information of the primary gaze network by unveiling gaze semantic difference.

- Our network achieves competitive performance over both within-domain and cross-domain tasks on MPIIFaceGaze, EyeDiap, Gaze360 and ETH-XGaze datasets.

## 2. Related Work

**Gaze estimation.** With the recent developments in deep learning, appearance-based gaze estimation methods have become the mainstream. Researchers explored various CNN-based architectures [6, 8, 50] to build the mapping between facial images and gaze directions. Zhang et al. [49] firstly proposed a CNN-based gaze estimation network and the well-known MPIIFaceGaze dataset. With the introduction of Transformer [36], the Vision Transformer-based structures have started to be applied to gaze estimation and achieved promising performance (e.g., GazeTR [7], oh et al. [29], SUGE [39]). In the recent years, researchers dedicated themselves to inventing generalized gaze estimation methods, which would show robust performance on unseen users. Several methods leveraged a gaze redirection strategy to extend the datasets for generalized gaze estimation [16, 44]. Cheng et al. [10] introduced a method of purifying gaze features to improve the networks generalization. Besides, some methods based on contrastive learning [41] and uncertainty learning [39, 53] also demonstrated remarkable generalizability. In this paper, we leverage CLIP to improve discriminability and generalization of the gaze estimation network.

**Pre-trained Vision-language Models.** Recently, the CLIP [31] trained on large-scale image-text pairs have attracted increasing attentions. Because of its powerful visual and semantic representation capabilities, CLIP has been transferred to various vision tasks, such as objection detection [37], semantic segmentation [55], and others [18, 25, 42]. Especially, CLIP also shows surprising capacities on quantified vision tasks, e.g., depth estimation [46, 47], 3D hand poses estimation [17], etc. Moreover, researchers were attempting to take advantages of the pre-trained CLIP to predict gaze directions. Wang et al. [38] designed a linguistic description generator to produce text signals with coarse gaze directional cues. And then a cross-attention condenser was designed to finely recalibrate the visual and text representations, enhancing the learning quality of gaze features. Yin et al. [45] designed a feature separation loss by employing CLIP text encoder to generate gaze distractors from diverse language descriptions, which aims at purifying the gaze-relevant feature via pushing away it from gaze-irrelevant features. In this paper, we adapt CLIP to gaze estimation with an innovative collaborative enhancing strategy, in which the CLIP is regarded as an assistance to enhance the obtained gaze features.

## 3. Methodology

To fully activate the potentials of CLIP to perceive gaze directions, we propose a novel Differential Contrastive Training (DCTrain) strategy, in which the CLIP is leveraged for unveiling gaze semantic differences of image-pairs. Accordingly, we propose a **Differential Contrastive Gaze Estimation network (DCGaze)** as shown in Figure 2 which consists of a Visual Appearance-aware branch and a Semantic Difference-aware branch. The former is essentially a primary gaze estimation network, while the latter is to encourage the Visual Appearance-aware branch to extract gaze-related features with the help of image-language contrastive learning.

### 3.1. Visual Appearance-aware Branch

The Visual Appearance-aware branch is composed of a Basic Appearance Feature Extractor and two innovative modules, namely a Adaptive Feature-refinement Unit (AFU) and a Double-head Gaze Regressor (DGR). The basic feature extractor captures the appearance feature of each facial image. The two proposed modules are designed to help extract informative and gaze-related appearance features.

#### 3.1.1. Basic Appearance Feature Extractor

We employ the remarkable CNN-Transformer architecture [7] as the basic structure, where a ResNet is firstly adopted to acquire feature maps  $f_i^{maps} \in \mathbb{R}^{W \times H \times C}$  of a given image  $x_i \in X$  where  $X = \{x_1, x_2, \dots, x_n\}$ . Then those feature maps are reshaped into  $W \times H$  patches  $f_i^p \in \mathbb{R}^{(W \times H) \times C}$ , which are treated as a series of  $C$ -dimensional visual tokens. After adding an extra learnable token  $f_i^{token} \in \mathbb{R}^{1 \times C}$ , which is used to aggregate the features of all the patches, we feed them into a Transformer with a learnable position embedding  $f_i^{pos} \in \mathbb{R}^{(1+W \times H) \times C}$ . Overall, we get the final primary appearance feature  $f_i^{pry} \in \mathbb{R}^{1 \times C}$  as Eq. (1).

$$f_i^{pry} = \text{Transformer}([f_i^{token}; f_i^p] + f_i^{pos})[0, :], \quad (1)$$

where  $[0, :]$  represents that the first row of the output feature maps is serving as the primary feature and  $[:]$  denotes the concatenation operation.

#### 3.1.2. Adaptive Feature-refinement Unit

It is well-known that CLIP trained on large-scale image-text pairs from the Internet have achieved excellent performance in various face-related downstream tasks, including age estimation [13], facial image editing [30], etc [32]. Those remarkable applications demonstrate that the visual encoder of CLIP has powerful abilities to characterize prior appearance information of facial images. Undoubtedly, this appearance information is always mixed by crucial information that is beneficial for gaze estimation and redundant information which may harm the accuracy. We hold an

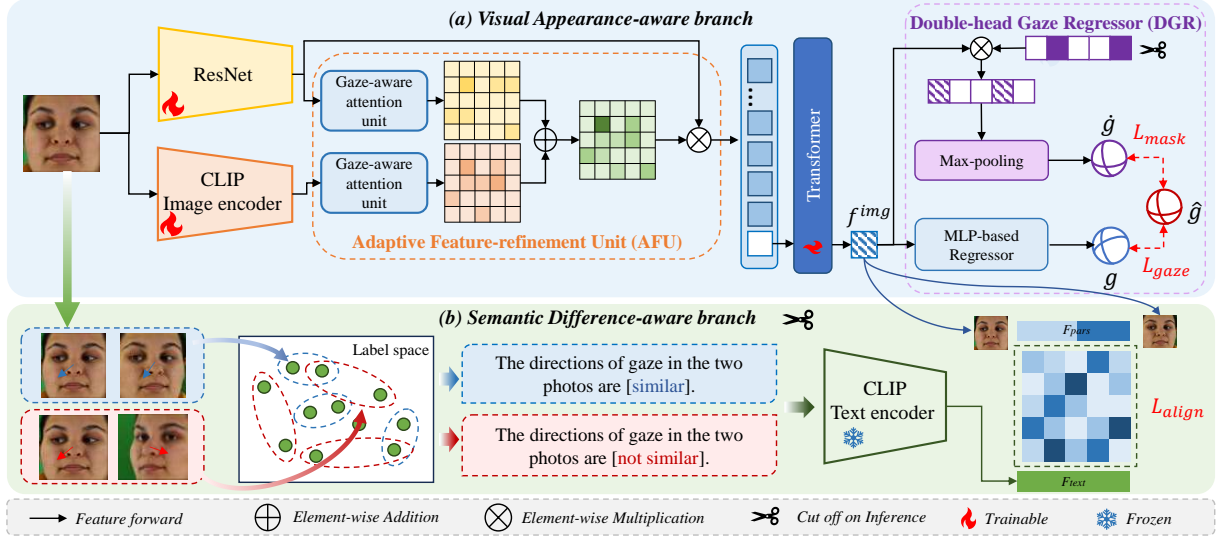


Figure 2. Framework of our proposed DCNet. It consists of two branch: Visual Appearance-aware branch and Semantic Difference-aware branch. In Visual Appearance-aware branch, the AFU is designed to adaptively enhance the gaze-related contents of primary appearance features with the guidance of the prior appearance features of CLIP’s image encoder. The DGR maps those enhanced features to final gazes via two regression heads. The Semantic Difference-aware branch selects several image-pairs from sample batch and gives each of them a textual prompt that describes their gaze differences. Then, the prompts are fed into CLIP’s text encoder to capture text embeddings, which are then aligned with enhanced appearance features obtained by our Visual Appearance-aware branch.

assumption that *the components present in both the primary appearance feature and the prior appearance feature from CLIP are the most important ones for gaze estimation*. Therefore, the Adaptive Feature-refinement Unit (AFU) is designed to dynamically enhance the gaze-related contents contained in the primary appearance features with the guidance of the prior appearance features from CLIP.

Firstly, a group of gaze-aware attention units are introduced to calculate the attention maps of the prior appearance features  $f_i^{clip}$  from CLIP image encoder and raw feature maps  $f_i^{maps}$  from Basic Appearance Feature Extractor, respectively (Eq. (2)).

$$\begin{aligned} M_i^{clip} &= \text{Softmax} \left( f_i^{clip} W_Q^{clip} (f_i^{clip} W_K^{clip})^T / \beta \right), \\ M_i^{gaze} &= \text{Softmax} \left( f_i^{maps} W_Q^{maps} (f_i^{maps} W_K^{maps})^T / \beta \right), \end{aligned} \quad (2)$$

where  $W_Q^{clip}$ ,  $W_K^{clip}$ ,  $W_Q^{maps}$ ,  $W_K^{maps}$  are learnable parameters of linear projections. The obtained attention maps  $M$  capture the respective dependencies between components of the two features, which could reveal the valuable parts of them.

And then, to further activate the key gaze-related components of the primary appearance features, we integrate the two attention maps and refine the primary feature map to an enhanced one (Eq. (3)). Intuitively, the integrated attention map acts as a mask that highlights the important

information involved in the primary appearance feature.

$$\hat{f}_i^{maps} = (M_i^{clip} + M_i^{gaze}) f_i^{maps}. \quad (3)$$

Then we feed the enhanced feature maps  $\hat{f}_i^{maps}$  into a Transformer to get an enhanced appearance feature  $f_i^{img}$  following the process of the Basic Appearance Feature Extractor as Eq. (1).

By thoroughly exploring the relationships between components of primary appearance features and prior appearance features, the AFU could identify the vital information that is correlated to gaze directions and thus encourages the primary gaze estimation model to obtain informative and gaze-related appearance features.

### 3.1.3. Double-head Gaze Regressor

Even with the enhanced features, the design of the regressor is also crucial for improving the model’s generalization ability. Existing methods [8, 50] typically use a simple MLP-based architecture to regress features into gaze directions. As discussed in the early work [2], the numerous parameters of MLP would easily overfit to gaze-irrelevant factors within the high-dimensional features during the mapping process. To mitigate the overfitting issues caused by MLP, we propose a Double-head Gaze Regressor (DGR). One of the regression head adopts the conventional MLP-based structure, which projects the enhanced gaze feature  $f_i^{img}$  to a final gaze direction as Eq. (4). Then we employ



the  $L_1$  loss (Eq. (4)) to minimize the discrepancy between the estimated gaze direction  $g_i$  and the ground truth  $\hat{g}_i$ ,

$$g_i = \text{MLP}(f_i^{\text{img}}), L_{\text{gaze}} = \frac{1}{N} \sum_{i=1}^N \|g_i - \hat{g}_i\|_1, \quad (4)$$

where  $N$  represents the number of image samples.

Inspired by the motivation of the dropout layers in neural networks [33], we design a masked regression head. Specifically, we construct a mask  $m_i \in \mathbb{R}^{1 \times C}$  with the same size as  $f_i^{\text{img}}$ , whose elements are either 0 or 1. The numbers of 0s and 1s in the mask are manually adjusted by a drop ratio. For example, if the  $f_i^{\text{img}}$  is a 32-dimensional vector and the drop ratio is set as 5/32, the mask would include five 0s and twenty-seven 1s with random positions. Then we take the Hadamard product of the masks with our enhanced gaze features  $f_i^{\text{img}}$  and get the masked features  $f_i^{\text{img}.m}$  (Eq. (5)).

$$f_i^{\text{img}.m} = f_i^{\text{img}} \circ M_i. \quad (5)$$

Next, we utilize the sampling method of max-pooling to directly map the high-dimensional masked features  $f_i^{\text{img}.m}$  to 2D gaze vectors  $\dot{g}_i$  without any parameters. Meanwhile, we also employ  $L_1$  loss ( $L_{\text{mask}}$  in Eq. (6)) to minimize the distance between the predicted gaze vector  $\dot{g}$  and the ground truth  $\hat{g}_i$ .

$$\dot{g}_i = \text{MaxPooling}(f_i^{\text{img}.m}), L_{\text{mask}} = \frac{1}{N} \sum_{i=1}^N \|\dot{g}_i - \hat{g}_i\|_1. \quad (6)$$

The DGR guides the model to focus on all the dimensions of the features rather than overfit on several dimensions without increasing the number of parameters, which could promote the generalization ability of our gaze regressor.

### 3.2. Semantic Difference-aware Branch

The Semantic Difference-aware branch is designed to implement the Differential Contrastive Training strategy. It aims to further enhance the extracted appearance features of the Visual Appearance-aware branch from the perspective of integrating gaze-related semantic information driven by the language-image alignment.

#### 3.2.1. Differential Gaze Prompts

As indicated in Introduction, the challenge lies in the connections between the infinite continuous gaze direction of each facial image and the restricted language sentences. Intuitively, it is easier to describe the difference of gazes between two facial images than to give individual description of the gaze in each image. Therefore, we design a series of differential gaze prompts, each of which refers to a language sentence describing the correlations of gaze directions between a pair of images.

Table 1. Design of the differential gaze prompts.

Template	$K$	Difference Interval	Grade Names
'The directions of gaze in the two photos are {Grade Name}'.	2	[0, 0.2)	'similar'
		[0.2, +∞)	'not similar'
	3	[0, 0.1)	'identical'
		[0.1, 0.2)	'similar'
		[0.2, +∞)	'not similar'
		[0, 0.1)	'identical'
	5	[0.1, 0.2)	'highly similar'
		[0.2, 0.3)	'moderately similar'
		[0.3, 0.5)	'slightly similar'
		[0.5, +∞)	'not similar'

To be specific, we pair each sample in a batch with every other one to form various image pairs and calculate their gaze differences with regards to their true gaze labels. The gaze difference is measured by the  $L_1$  distances between the gaze directions of the image pair. Then, we categorize these image pairs into  $K$  semantic similarity levels according to their gaze differences, and each level is attributed with a semantic grade name  $t_i^{\text{grade}}$ , e.g., 'identical', 'similar', 'not similar'. Subsequently, a differential gaze prompt  $T_i$  of each image pair is generated via combining a designed template  $t_i^{\text{template}}$ : 'The directions of gaze in the two photos are {grade name}.' with a corresponding semantic grade  $t_i^{\text{grade}}$  (Eq. (7)). For instance, if  $K$  is set to 2, all the selected image pairs are divided into 'similar' and 'not similar' groups. The image pairs with gaze differences that are from 0 to 0.2 are assigned into the 'similar' grade, while image pairs with gaze differences that are over 0.2 are allocated to the 'not similar' grade. The designed differential gaze prompts and their corresponding specific gaze differences are shown in Table 1. And we evaluate the performance of different designs in Experiments.

#### 3.2.2. Differential Contrastive Training

Given the differential gaze prompts  $T_i$ , a pre-trained CLIP text encoder is employed to encode it into a text embedding ( $f_i^{\text{text}}$ ) as Eq. (7),

$$T_i = [t_i^{\text{template}}, t_i^{\text{grade}}], f_i^{\text{text}} = \text{TextEncoder}(T_i). \quad (7)$$

To further enhance the extracted appearance features, we innovatively realize a visual-semantic alignment between the CLIP text encoder and the Visual Appearance-aware branch. Ideally, the semantic enhanced visual features of facial images should be aligned with the above text embeddings. In other words, the compatibilities between visual embeddings of image-pairs and the text embeddings of their corresponding differential gaze prompts should be higher than the compatibilities between image-pairs and other misaligned descriptions. The visual embeddings of image pairs

are derived from the concatenated features of the above visual branch of the selected two images, as Eq. (8),

$$f_i^{pair} = \text{MLP}([f_{i1}^{img}; f_{i2}^{img}]). \quad (8)$$

A language-driven contrastive loss is thus designed as Eq. (9),

$$L_{align} = -\frac{1}{N_p} \sum_{i=1}^{N_p} \log \frac{\exp(f_i^{text} \cdot f_i^{pair} / \tau)}{\sum_{j=1}^{N_p} \exp(f_i^{text} \cdot f_j^{pair} / \tau)} - \frac{1}{N_p} \sum_{i=1}^{N_p} \log \frac{\exp(f_i^{pair} \cdot f_i^{text} / \tau)}{\sum_{j=1}^{N_p} \exp(f_i^{pair} \cdot f_j^{text} / \tau)}, \quad (9)$$

where  $N_p$  is the number of selected image-pairs in one batch and  $\tau$  is a temperature hyperparameter. In our experiments, for each facial image in a sample batch, all the remaining samples in this batch are selected to constitute image pairs with it. Thus we can obtain  $N_p = (N_b - 1) \times (N_b - 1)$  pairs in each sample batch and then partition them into  $K$  semantic grades according to their true gaze labels.  $N_b$  denotes the number of samples in a training batch.

By minimizing the  $L_{align}$ , our Visual Appearance-aware branch could be endowed with the ability to perceive gaze semantic difference, thus takes full advantages of the gaze-related semantic information. The innovations could be illustrated as follows. On the one hand, rather than extracting features from individual images, by comparing different facial images, interactions of gaze between them will be characterized, which benefits the extraction of robust gaze-related features. On the other hand, the proposed Differential Contrastive Training strategy essentially simplifies the target words that the CLIP needs to understand by replacing unfamiliar phrases, e.g., ‘[0.54 (pitch), -0.20 (yaw)]’ with familiar ones, e.g., ‘similar’, ‘not similar’ (Figure 1). Moreover, the continuous gaze labels are transformed into discrete similarity levels of a pair of gazes. These could cleverly address the challenges that hinder the applications of CLIP in gaze estimation as discussed in Introduction. Eventually, by realizing the language-image alignment, the consistency between extracted features and gaze labels is maintained derivatively. Differential Contrastive Training helps to learn robust and pure gaze-related features.

### 3.3. Optimization and Inference

In training stage, our network is optimized by minimizing the total loss function as follows:

$$L_{total} = L_{gaze} + \alpha L_{mask} + \beta L_{align}, \quad (10)$$

where  $\alpha$  and  $\beta$  are hyperparameters to balance the losses. The text encoder of Semantic Difference-aware branch is frozen and the parameters of the primary gaze estimation network consisting of AFU and DGR should be updated.

Table 2. Performance on within-domain tasks. Results reported are angular errors in degrees. **Bold** and underline indicate the best and the second best result.

Method	Refs	$\mathcal{D}_M$	$\mathcal{D}_D$	$\mathcal{D}_G$
Itracker [24]	2016 CVPR	6.20	9.93	-
FullFace [50]	2017 CVPRW	4.93	6.53	14.99
RT-Gene [14]	2018 ECCV	4.30	5.90	-
Dilated-Net [6]	2018 ACCV	4.42	6.19	13.73
Gaze360 [22]	2019 ICCV	4.06	5.36	11.04
FAR-Net [9]	2020 TIP	4.30	5.71	-
CA-Net [8]	2020 AAAI	4.27	5.27	11.20
GazeTR [7]	2021 ICPR	4.00	5.17	10.62
Oh et al. [29]	2022 CVPRW	4.04	5.25	10.70
SUGE [39]	2024 AAAI	4.01	<u>5.04</u>	<b>10.51</b>
<b>DCGaze*</b>	<b>Ours</b>	<u>3.76</u>	5.15	10.58
<b>DCGaze</b>	<b>Ours</b>	<b>3.71</b>	<b>4.97</b>	<u>10.54</u>

During the inference stage, the Semantic Differential-aware branch and the masked regression head of DGR should be cut off. In other words, we believe that with the Differential Contrastive Training, the primary gaze estimation model is capable of extracting informative gaze-related features. Therefore, the facial images are fed into the Basic Appearance Feature Extractor and the AFU to obtain the enhanced appearance features. Finally, we employ the MLP-based head to project the enhanced features into final gaze directions. Moreover, some existing studies [43] have also employed differential ideas to remove gaze-irrelevant factors from extracted gaze features. However, they still need to implement the differential calculations during the inference stage, whose predicted results heavily rely on the selected reference samples. Superior to them, our proposed differential module is regarded as an assistant line, whose mission is to encourage the primary network to extract a robust feature that contains gaze-related information. Therefore, we achieve a simpler and more direct inference stage.

## 4. Experiments

### 4.1. Datasets and settings

Our method is evaluated on four popular gaze estimation datasets, which are MPIIFaceGaze ( $\mathcal{D}_M$ ) [51], EyeDiap ( $\mathcal{D}_D$ ) [15], Gaze360 ( $\mathcal{D}_G$ ) [22] and ETH-XGaze ( $\mathcal{D}_E$ ) [52] over within and cross-domain tasks. More details of datasets refer to supplementary materials.

For within-domain evaluation, the experiments are conducted on MPIIFaceGaze, EyeDiap and Gaze360 datasets. We perform leave-one-person-out evaluation on MPIIFaceGaze dataset and four-folder cross validation on EyeDiap dataset. As for the Gaze360 dataset, after removing the images without frontal faces, we select 84,902 images of 54 subjects for training and 16,000 images of 15 subjects

Table 3. Performance on cross-domain tasks.  $|\mathcal{D}_t|$ : the number of samples for fine-tuning or co-training. **Bold** and underline indicate the best and the second best result.

Methods	Refs	$ \mathcal{D}_t $	$\mathcal{D}_E \rightarrow \mathcal{D}_M$	$\mathcal{D}_E \rightarrow \mathcal{D}_D$	$\mathcal{D}_G \rightarrow \mathcal{D}_M$	$\mathcal{D}_G \rightarrow \mathcal{D}_D$
ADDA [34]	2017 CVPR	500	6.65	8.24	6.27	9.53
GazeAdv [20]	2019 CVPRW	100	6.36	7.62	7.54	8.43
Gaze360 [22]	219 ICCV	100	6.24	7.47	7.17	7.66
DAGEN [19]	2020 ACCV	500	5.73	6.77	7.38	8.00
UMA [5]	2020 CVPR	100	7.52	12.37	8.51	19.32
PnP-GA [27]	2021 ICCV	10	5.53	5.87	6.18	7.92
CRGA [40]	2022 CVPR	0	5.48	5.66	5.89	6.49
RUDA [3]	2022 CVPR	100	5.70	7.52	6.20	7.02
DCUA [48]	2024 TMM	100	7.31	5.95	5.59	6.40
CLIP-Gaze [45]	2024 AAAI	100	4.45	<b>5.27</b>	4.94	5.60
PnP-GA <sup>+</sup> [26]	2024 TPAMI	10	5.34	5.73	6.10	7.62
<b>DCGaze*</b>	<b>Ours</b>	100	<b>4.37</b>	<u>5.36</u>	<b>4.83</b>	<b>5.49</b>
<b>DCGaze</b>	<b>Ours</b>	100	6.00	6.01	5.25	6.21

for testing. For cross-domain evaluation, the Gaze360 and ETH-XGaze datasets are treated as source domain for training, while MPIIFaceGaze and EyeDiap are target ones for testing. Thus, we evaluate our method on four cross-domain tasks:  $\mathcal{D}_E \rightarrow \mathcal{D}_M$ ,  $\mathcal{D}_E \rightarrow \mathcal{D}_D$ ,  $\mathcal{D}_G \rightarrow \mathcal{D}_M$ ,  $\mathcal{D}_G \rightarrow \mathcal{D}_D$ .

## 4.2. Implementation details

We employ the pre-trained RN50 CLIP for the backbones of our Semantic Difference-aware branch and AFU, which consists of a ResNet50-based image encoder and a Transformer-based text encoder. During the training stage, the text encoder is frozen, while the image encoder would be fine-tuned.

In the within-domain evaluation, the Basic Appearance Feature Extractor is composed of a ResNet18 and a 6-layer Transformer. Given the  $224 \times 224$  input images,  $7 \times 7 \times 32$  feature maps are generated from ResNet18 and then fed into a 6-layer Transformer with 8-head self-attention mechanism. Finally, we get a 32-dimensional image feature. In the cross-domain evaluation, the Transformer is replaced by a 3-layer MLP to mitigate the overfitting issues. The weighted factors  $\alpha$  and  $\beta$  in Eq. (10) are important parameters in our method. In the current experiments, they are set to (0.1, 0.1) for both within-domain tasks and cross-domain tasks.

## 4.3. Comparison with State-of-the-art Methods

We compare our approach with the SOTAs. The results are shown in Table 2 and Table 3. The reported results come from [44] or their original papers. **DCGaze** denotes our full model. **DCGaze\*** denotes the sub-model that removes the AFU.

**Performance on within-domain tasks.** We roughly classify the compared methods into CNN-based methods

(upper part of Table 2) and Transformer-based methods (bottom part of Table 2). As the results shown in Table 2, our approach outperforms all within-domain methods on the MPIIFaceGaze and EyeDiap datasets. It also achieves performance comparable to the SUGE [39] on Gaze360 dataset. The results prove that our DCGaze can strengthen the gaze-related appearance and semantic information in gaze features, leading to higher accuracy.

**Performance on cross-domain tasks.** To further demonstrate the generalizability of our method, we conduct experiments on unsupervised domain adaptation (UDA) tasks. In UDA settings, the models are trained on source domain while testing on unseen target domain.  $|\mathcal{D}_t|$  samples from target domain could be randomly selected for further adaptation (fine-tuning or co-training). As the results shown in the Table 3, our sub-model DCGaze\* achieves the best performance on  $\mathcal{D}_E \rightarrow \mathcal{D}_M$ ,  $\mathcal{D}_G \rightarrow \mathcal{D}_M$  and  $\mathcal{D}_G \rightarrow \mathcal{D}_D$  tasks. Those results also demonstrate the effectiveness of our proposed Differential Contrastive Training strategy.

## 4.4. Ablation Study

### 4.4.1. Effectiveness of the Differential Contrastive Training strategy.

We treat the Semantic Difference-aware branch along with our Differential Contrastive Training strategy as a plug-and-play module, and evaluate its properties via integrating it into various basic gaze estimation models. The results are shown in Table 4 and Table 5. our DCTrain strategy could bring performance improvements to those various basic models. It demonstrates that DCTrain does develop the potentials of the pre-trained CLIP in boosting gaze estimation performance.

Table 4. Effectiveness of the Differential Contrastive Training on within-domain tasks.

Model	MPII	EyeDiap	Gaze360
Resnet18	4.15	5.67	12.40
Resnet18+DCTrain	4.15	<b>5.63</b>	<b>12.09</b>
Resnet50	4.30	5.67	11.77
Resnet50+DCTrain	<b>4.19</b>	<b>5.59</b>	<b>11.68</b>
GazeTR	4.13	5.23	10.76
GazeTR+DCTrain	<b>3.73</b>	<b>5.15</b>	<b>10.50</b>

### 4.4.2. Ablation Study of Proposed Modules

To investigate the effectiveness of each proposed component, we compare the performance of some degraded models on both within and cross-domain tasks. Based on the fully model, we remove one proposed component each time and get the results in Table 6 and in Table 7. The 1st. rows refer the baseline models. In within-domain evaluation, the baseline model consists of a CNN-Transformer-

Table 5. Effectiveness of the Differential Contrastive Training on cross-domain tasks.

Model	$\mathcal{D}_E \rightarrow \mathcal{D}_M$	$\mathcal{D}_E \rightarrow \mathcal{D}_D$	$\mathcal{D}_G \rightarrow \mathcal{D}_M$	$\mathcal{D}_G \rightarrow \mathcal{D}_D$
Resnet18	5.56	6.83	8.81	8.92
Resnet18+DCTrain	<b>5.55</b>	<b>6.41</b>	<b>8.02</b>	<b>8.60</b>
Resnet50	5.25	6.51	4.93	5.41
Resnet50+DCTrain	<b>5.21</b>	<b>6.33</b>	<b>4.87</b>	<b>5.36</b>

Table 6. Ablation study results of proposed components on within-domain tasks.

DCTrain	AFU	DGR	MPII	EyeDiap	Gaze360
-	-	-	4.13	5.23	10.76
-	✓	✓	3.77	5.06	10.65
✓	-	✓	3.76	5.15	10.58
✓	✓	-	3.77	5.18	10.58
✓	✓	✓	<b>3.71</b>	<b>4.97</b>	<b>10.54</b>

based Feature Extractor and an MLP-based regressor. In cross-domain evaluation, the Transformer part of the Feature Extractor is replaced by a 3-layer MLP. In within-domain tasks, no matter which component is invalidated, the performance decreases. This proves the importance of each of them. 1) By comparing the 2<sup>nd</sup>. rows with the 5<sup>th</sup>. rows (full model), it demonstrates that the Semantic Difference-aware branch can help the visual branch capture robust and pure gaze-related features via image-text alignment. 2) By comparing the 4<sup>th</sup>. rows with the 5<sup>th</sup>. rows, the DGR has been proven effective in reducing degrees of freedom and improving generalizability. 3) By comparing the 3<sup>rd</sup>. rows with the 5<sup>th</sup>. rows, AFU could bring improvements to within-domain tasks but lead a decline in performance for cross-domain ones. We analyze the possible reasons. CLIP is likely to encode scene contexts (e.g., image resolution, illumination, etc.) into its obtained appearance embeddings. For cross-domain tasks, the test samples own significantly different environments with training ones. Thus the AFU is more adept at capturing the scene information of the source domain, which may disturb the estimation of disjoint target samples.

#### 4.4.3. Analysis of Differential Gaze Prompts

In this section, we evaluate our DCGaze under different prompt designs (Table 8). Firstly, we vary the number of grade prompts  $K$  from 2 to 5. The results show that increasing the number of grades can better help the model to identify the subtle gaze differences between facial images, leading to better feature representations. However, the more levels there are, the more difficult manual designs of textual prompts become. Thus, we select 5 grades in our experiments. Secondly, we explore different strategies to describe

Table 7. Ablation study results of proposed components on cross-domain tasks.

DCTrain	AFU	DGR	$\mathcal{D}_E \rightarrow \mathcal{D}_M$	$\mathcal{D}_E \rightarrow \mathcal{D}_D$	$\mathcal{D}_G \rightarrow \mathcal{D}_M$	$\mathcal{D}_G \rightarrow \mathcal{D}_D$
-	-	-	7.14	7.83	7.10	8.59
-	✓	✓	6.47	6.20	5.65	6.60
✓	-	✓	<b>4.37</b>	<b>5.36</b>	<b>4.83</b>	<b>5.49</b>
✓	✓	-	6.48	6.75	5.97	6.89
✓	✓	✓	6.21	6.05	5.63	6.33

these prompts. To be specific, we use different words for each differential grade name or propose a learnable prompt template following the CoOp method [54]. Two main observations could be concluded from the comparisons. 1) The manual prompts combining with degree adverbs can convey more precise semantic information, which lead to better results. 2) The learnable prompt template performs worse than the fixed one, whose possible reason is that the fixed prompt template could clearly describe the gaze difference between images while the learnable one may introduce some noise during the learning process.

#### 4.4.4. Analysis of Feature Refinement Strategy

As discussed in Section 3.1.2, a novel Adaptive Feature-refinement Unit is proposed to dynamically enhance the gaze-related contents of primary appearance features. In order to evaluate the properties of this unit, we compare it with several commonly used feature fusion methods on within-domain tasks.

- ‘Concatenation: We concatenate the prior appearance feature of CLIP and the primary appearance feature, and feed them into a fully connected layer to preserve the feature dimensions.
- ‘Cross-Attention: We treat the primary appearance feature  $f_{pry}$  as query  $Q$  and the prior appearance feature  $f_{clip}$  as key  $K$  and value  $V$ . The final fused features  $f^{img}$  is computed as Eq. (11):

$$Q_{pry} = f^{pry}W_Q, K_{clip} = f^{clip}W_K, V_{clip} = f^{clip}W_V, \\ f^{img} = \text{Softmax}(Q_{pry}K_{clip}^T/\beta)V_{clip}. \quad (11)$$

- ‘Gated Information Fusion: Following [1], the prior appearance feature  $f^{clip}$  is processed by a sigmoid operation to generate a mask, which is used to activate the primary appearance feature  $f^{img}$  via Hadamard product. The detailed process refers to Eq. (12):

$$f^{img} = f^{pry} \circ \text{Sigmoid}(f^{clip}), \quad (12)$$

As shown in Table 9, our AFU consistently outperforms all compared methods, which indicates that it could effectively highlight vital appearance information to enhance the primary gaze feature.



Table 8. Analysis of differential gaze prompts. The fixed template is ‘The directions of gaze in the two photos are  $\{Grade\ Name\}$ .’

$K$	Template	Grade Names	MPII	EyeDiap	Gaze360
2	fixed	‘similar’, ‘not similar’	3.73	5.08	10.56
3		‘identical’, ‘similar’, ‘not similar’	3.82	5.13	10.60
5		‘almost identical’, ‘extremely similar’, ‘similar’, ‘a little similar’, ‘different’	3.75	5.02	10.58
5	fixed	‘identical’, ‘highly similar’, ‘moderately similar’, ‘slightly similar’, ‘not similar’	<b>3.71</b>	<b>4.97</b>	10.54
5	learnable	‘identical’, ‘highly similar’, ‘moderately similar’, ‘slightly similar’, ‘not similar’	3.81	5.09	<b>10.53</b>

Table 9. Analysis of feature fusion strategy.

Fusion methods	MPII	EyeDiap	Gaze360
Concatenation	3.77	5.29	10.57
Cross-Attention	3.80	5.21	10.56
Gated Information Fusion	3.78	5.13	10.59
<b>AFU (proposed)</b>	<b>3.71</b>	<b>4.79</b>	<b>10.54</b>

## 4.5. More Discussion <sup>1</sup>

### 4.5.1. Visualization of Obtained Gaze Features

To quantitatively demonstrate the advantages of our enhanced gaze features, we visualize the distribution of the training samples of Gaze360 and ETH-XGaze datasets by t-SNE [35], following [41]. We select all the training samples of Gaze360 dataset and randomly select 10000 training samples from ETH-XGaze dataset. In the scatter plot, the samples are clustered by KMeans [21] according to their gaze labels, so that the samples with similar gaze directions share similar colors. The feature distributions of the Baseline and our DCGaze are shown in Figure 3. As shown in the left figure, the sample points of baseline are scattered in a chaotic manner. By contrast, feature points of our enhanced features are distributed in an organized way, in which the features with similar gaze directions are clustered and can be regressed to similar gazes. It demonstrates our enhanced features being purified gaze-related ones, which effectively improve the discriminability and generalization.

### 4.5.2. Visualization of Estimated Gazes

We further visualize the true gazes (green arrow), the predicted gaze directions of baseline (blue arrow) and the predicted gaze directions of DCGaze (red arrow). We select several test samples of Gaze360 dataset in different conditions including extreme head poses, dark illumination and low quality. The visualized results are shown in Figure 4. Compared to baseline method, the estimated results of our method are closer to ground truths in most conditions.

<sup>1</sup>In supplementary materials, we conduct more experiments to evaluate the properties of our proposed modules.

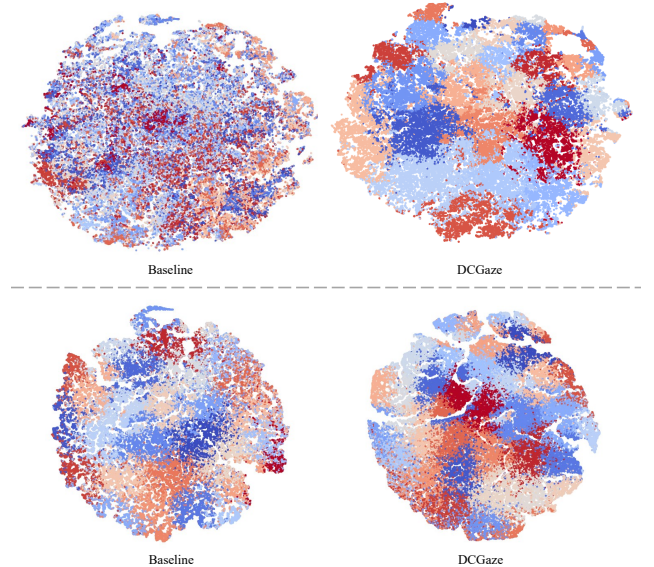


Figure 3. Visualization of obtained gaze features of Gaze360 (upper) and ETH-XGaze (bottom) datasets.

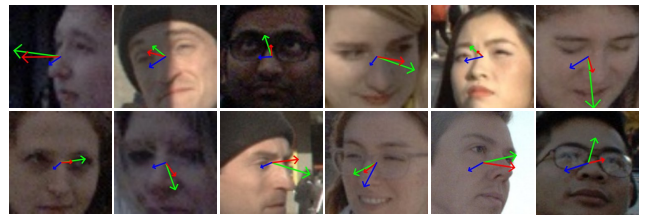


Figure 4. Visualization of estimated gazes.

## 5. Conclusion

In this paper, we have proposed a novel Differential Contrastive Gaze Estimation network (DCGaze) for gaze estimation, which leverages the powerful capabilities of the pre-trained CLIP to improve the representation capacity of a primary network by a novel Differential Contrastive Training strategy. Firstly, in the Visual Appearance-aware branch, the AFU and DGR have been proposed to help the primary gaze estimation model to capture informative and gaze-related features. Besides, to realize the Differential Contrastive Training, the Semantic Difference-aware branch has constructed image-pairs and designed differen-

tial gaze prompt for each of them. Through visual-semantic alignment, the primary gaze estimation network has been endowed with the ability of extracting robust and pure gaze-related features. In extensive experiments, DCGaze has achieved remarkable performance on both within-domain tasks and cross-domain tasks. *Limitation:* DCGaze is not a lightweight model, which would limit its deployment on edge devices in real application scenarios. Therefore, in the future, we would keep improving DCGaze in terms of reducing its scalability while maintaining the precision of prediction.<sup>2</sup>

## References

- [1] John Arevalo, Tamar Solorio, Manuel Montes y Gómez, and Fabio A. González. Gated multimodal units for information fusion. *ArXiv*, abs/1702.01992, 2017. 8
- [2] Yiwei Bao and Feng Lu. From feature to gaze: A generalizable replacement of linear layer for gaze estimation. In *2024 IEEE/CVF Conference on Computer Vision and Pattern Recognition (CVPR)*, pages 1409–1418, 2024. 4
- [3] Yiwei Bao, Yunfei Liu, Haoifei Wang, and Feng Lu. Generalizing gaze estimation with rotation consistency. In *2022 IEEE/CVF Conference on Computer Vision and Pattern Recognition (CVPR)*, pages 4197–4206. IEEE, 2022. 7
- [4] Alisa Burova, John Mäkelä, Jaakko Hakulinen, Tuuli Keskinen, Hanna Heinonen, Sanni Siltanen, and Markku Turunen. Utilizing vr and gaze tracking to develop ar solutions for industrial maintenance. *Proceedings of the 2020 CHI Conference on Human Factors in Computing Systems*, 2020. 1
- [5] Minjie Cai, Feng Lu, and Yoichi Sato. Generalizing hand segmentation in egocentric videos with uncertainty-guided model adaptation. In *2020 IEEE/CVF Conference on Computer Vision and Pattern Recognition (CVPR)*, pages 14380–14389, 2020. 7
- [6] Zhaokang Chen and Bertram E. Shi. Appearance-based gaze estimation using dilated-convolutions. In *Asian Conference on Computer Vision*, pages 309–324. Springer International Publishing, 2019. 3, 6
- [7] Yihua Cheng and Feng Lu. Gaze estimation using transformer. In *International Conference on Pattern Recognition*, pages 3341–3347. IEEE, 2022. 3, 6
- [8] Yihua Cheng, Shiyao Huang, Fei Wang, Chen Qian, and Feng Lu. A coarse-to-fine adaptive network for appearance-based gaze estimation. In *Proceedings of the AAAI Conference on Artificial Intelligence*, pages 10623–10630, 2020. 3, 4, 6
- [9] Yihua Cheng, Xucong Zhang, Feng Lu, and Yoichi Sato. Gaze estimation by exploring two-eye asymmetry. *Transactions on Image Processing*, 29:5259–5272, 2020. 6
- [10] Yihua Cheng, Yiwei Bao, and Feng Lu. Puregaze: Purifying gaze feature for generalizable gaze estimation. In *Proceedings of the AAAI Conference on Artificial Intelligence*, pages 436–443, 2022. 3
- [11] Yihua Cheng, Yaning Zhu, Zongji Wang, Hongquan Hao, Yongwei Liu, Shiqing Cheng, Xi Wang, and Hyung Jin Chang. What do you see in vehicle? comprehensive vision solution for in-vehicle gaze estimation. In *2024 IEEE/CVF Conference on Computer Vision and Pattern Recognition (CVPR)*, pages 1556–1565, 2024. 1
- [12] Mehdi Cherti, Romain Beaumont, Ross Wightman, Mitchell Wortsman, Gabriel Ilharco, Cade Gordon, Christoph Schuhmann, Ludwig Schmidt, and Jenia Jitsev. Reproducible Scaling Laws for Contrastive Language-Image Learning. In *2023 IEEE/CVF Conference on Computer Vision and Pattern Recognition (CVPR)*, pages 2818–2829. IEEE, 2023. 1
- [13] Yao Du, Qiang Zhai, Weihang Dai, and Xiaomeng Li. Teach clip to develop a number sense for ordinal regression. *ArXiv*, abs/2408.03574, 2024. 3
- [14] Tobias Fischer, Hyung Jin Chang, and Yiannis Demiris. Rt-gene: Real-time eye gaze estimation in natural environments. In *European Conference on Computer Vision*, page 339357. Springer-Verlag, 2018. 6
- [15] Kenneth Alberto Funes Mora, Florent Monay, and Jean-Marc Odobez. EYEDIAP: A database for the development and evaluation of gaze estimation algorithms from RGB and RGB-D cameras. In *Proceedings of the Symposium on Eye Tracking Research and Applications*, pages 255–258. ACM, 2014. 6
- [16] Yaroslav Ganin, Daniil Kononenko, Diana Sungatullina, and Victor Lempitsky. DeepWarp: Photorealistic Image Resynthesis for Gaze Manipulation. In *European Conference on Computer Vision*, pages 311–326. Springer International Publishing, 2016. 3
- [17] Shaoxiang Guo, Qing Cai, Lin Qi, and Junyu Dong. CLIP-Hand3D: Exploiting 3D Hand Pose Estimation via Context-Aware Prompting. *Proceedings of the 31st ACM International Conference on Multimedia*, 2023. 1, 3
- [18] Yixin Guo, Yu Liu, Jianghao Li, Weimin Wang, and Qi Jia. Unseen no more: Unlocking the potential of clip for generative zero-shot hoi detection. In *Proceedings of the 32nd ACM International Conference on Multimedia*, pages 1711–1720, 2024. 3
- [19] Zidong Guo, Zejian Yuan, Chong Zhang, Wanchao Chi, Yonggen Ling, and Shenghao Zhang. Domain adaptation gaze estimation by embedding with prediction consistency. In *Asian Conference on Computer Vision*, page 292307, Berlin, Heidelberg, 2020. Springer-Verlag. 7
- [20] Zidong Guo, Zejian Yuan, Chong Zhang, Wanchao Chi, Yonggen Ling, and Shenghao Zhang. Domain Adaptation Gaze Estimation by Embedding with Prediction Consistency. In *Asian Conference on Computer Vision*, pages 292–307. Springer International Publishing, 2021. 7
- [21] Abiodun M. Ikotun, Absalom E. Ezugwu, Laith Abualigah, Belal Abuhaija, and Jia Heming. K-means clustering algorithms: A comprehensive review, variants analysis, and advances in the era of big data. *Information Sciences*, 622: 178–210, 2023. 9
- [22] Petr Kellnhofer, Adria Recasens, Simon Stent, Wojciech Matusik, and Antonio Torralba. Gaze360: Physically Unconstrained Gaze Estimation in the Wild. In *Proceedings of the*

<sup>2</sup>In supplementary materials, we discuss the scalability of DCGaze compared to other methods.

- IEEE/CVF International Conference on Computer Vision*, pages 6911–6920. IEEE, 2019. 6, 7
- [23] Robert Konrad, Anastasios Angelopoulos, and Gordon Wetstein. Gaze-contingent ocular parallax rendering for virtual reality. *ACM Trans. Graph.*, 39(2), 2020. 1
- [24] Kyle Krafka, Aditya Khosla, Petr Kellnhofer, Harini Kannan, Suchendra Bhandarkar, Wojciech Matusik, and Antonio Torralba. Eye tracking for everyone. In *2016 IEEE/CVF Conference on Computer Vision and Pattern Recognition (CVPR)*, pages 2176–2184, 2016. 6
- [25] Liunian Harold Li, Pengchuan Zhang, Haotian Zhang, Jianwei Yang, Chunyuan Li, Yiwu Zhong, Lijuan Wang, Lu Yuan, Lei Zhang, Jenq-Neng Hwang, Kai-Wei Chang, and Jianfeng Gao. Grounded Language-Image Pre-training. In *2022 IEEE/CVF Conference on Computer Vision and Pattern Recognition (CVPR)*, pages 10955–10965. IEEE, 2022. 3
- [26] Ruicong Liu, Yunfei Liu, Haofer Wang, and Feng Lu. Pnp-ga+: Plug-and-play domain adaptation for gaze estimation using model variants. *IEEE Transactions on Pattern Analysis and Machine Intelligence*, 46(5):3707–3721, 2024. 7
- [27] Yunfei Liu, Ruicong Liu, Haofer Wang, and Feng Lu. Generalizing Gaze Estimation with Outlier-guided Collaborative Adaptation. In *Proceedings of the IEEE/CVF International Conference on Computer Vision*, pages 3815–3824. IEEE, 2021. 7
- [28] Callum Mole, Jami Pekkanen, William E. A. Sheppard, Gustav Markkula, and Richard M. Wilkie. Drivers use active gaze to monitor waypoints during automated driving. *Scientific Reports*, 11(1):263, 2021. 1
- [29] Jun O Oh, Hyung Jin Chang, and Sang-Il Choi. Self-attention with convolution and deconvolution for efficient eye gaze estimation from a full face image. In *2022 IEEE/CVF Conference on Computer Vision and Pattern Recognition Workshops (CVPRW)*, pages 4988–4996, 2022. 3, 6
- [30] Or Patashnik, Zongze Wu, Eli Shechtman, Daniel Cohen-Or, and Dani Lischinski. StyleCLIP: Text-Driven Manipulation of StyleGAN Imagery. In *Proceedings of the IEEE/CVF International Conference on Computer Vision*, pages 2065–2074. IEEE, 2021. 3
- [31] Alec Radford, Jong Wook Kim, Chris Hallacy, Aditya Ramesh, Gabriel Goh, Sandhini Agarwal, Girish Sastry, Amanda Askell, Pamela Mishkin, Jack Clark, Gretchen Krueger, and Ilya Sutskever. Learning transferable visual models from natural language supervision. In *International Conference on Machine Learning*, 2021. 1, 3
- [32] Shuai Shen, Wanhua Li, Xiaobing Wang, Dafeng Zhang, Zhezhu Jin, Jie Zhou, and Jiwen Lu. CLIP-Cluster: CLIP-Guided Attribute Hallucination for Face Clustering. In *Proceedings of the IEEE/CVF International Conference on Computer Vision*, pages 20729–20738. IEEE, 2023. 3
- [33] Nitish Srivastava, Geoffrey Hinton, Alex Krizhevsky, Ilya Sutskever, and Ruslan Salakhutdinov. Dropout: A simple way to prevent neural networks from overfitting. *J. Mach. Learn. Res.*, 15(1):1929–1958, 2014. 5
- [34] Eric Tzeng, Judy Hoffman, Kate Saenko, and Trevor Darrell. Adversarial Discriminative Domain Adaptation. In *2017 IEEE/CVF Conference on Computer Vision and Pattern Recognition (CVPR)*, pages 2962–2971. IEEE, 2017. 7
- [35] Laurens van der Maaten and Geoffrey Hinton. Visualizing Data using t-SNE. *Journal of Machine Learning Research*, 9 (86):2579–2605, 2008. 9
- [36] Ashish Vaswani, Noam Shazeer, Niki Parmar, Jakob Uszkoreit, Llion Jones, Aidan N Gomez, ukasz Kaiser, and Illia Polosukhin. Attention is all you need. In *Neural Information Processing Systems*. Curran Associates, Inc., 2017. 3
- [37] Vidit Vedit, Martin Engilberge, and Mathieu Salzmann. CLIP the Gap: A Single Domain Generalization Approach for Object Detection. In *2023 IEEE/CVF Conference on Computer Vision and Pattern Recognition (CVPR)*, pages 3219–3229. IEEE, 2023. 3
- [38] Jun Wang, Hao Ruan, Mingjie Wang, Chuanghui Zhang, Huachun Li, and Jun Zhou. GazeCLIP: Towards enhancing gaze estimation via text guidance. *ArXiv*, abs/2401.00260, 2023. 2, 3
- [39] Shijing Wang and Yaping Huang. Suppressing Uncertainty in Gaze Estimation. In *Proceedings of the AAAI Conference on Artificial Intelligence*, pages 5581–5589, 2024. 3, 6, 7
- [40] Yaoming Wang, Yangzhou Jiang, Jin Li, Bingbing Ni, Wenrui Dai, Chenglin Li, Hongkai Xiong, and Teng Li. Contrastive regression for domain adaptation on gaze estimation. In *2022 IEEE/CVF Conference on Computer Vision and Pattern Recognition (CVPR)*, pages 19354–19363, 2022. 7
- [41] Yaoming Wang, Yangzhou Jiang, Jin Li, Bingbing Ni, Wenrui Dai, Chenglin Li, Hongkai Xiong, and Teng Li. Contrastive Regression for Domain Adaptation on Gaze Estimation. In *2022 IEEE/CVF Conference on Computer Vision and Pattern Recognition (CVPR)*, pages 19354–19363. IEEE, 2022. 3, 9
- [42] Yao Wu, Mingwei Xing, Yachao Zhang, Yuan Xie, and Yanyun Qu. Clip2uda: Making frozen clip reward unsupervised domain adaptation in 3d semantic segmentation. In *Proceedings of the 32nd ACM International Conference on Multimedia*, pages 8662–8671, 2024. 3
- [43] Lifan Xia, Yong Li, Xin Cai, Zhen Cui, Chunyan Xu, and Antoni B. Chan. Collaborative contrastive learning for cross-domain gaze estimation. *Pattern Recognition*, 161:111244, 2025. 6
- [44] Mingjie Xu and Feng Lu. Gaze from Origin: Learning for Generalized Gaze Estimation by Embedding the Gaze Frontalization Process. In *Proceedings of the AAAI Conference on Artificial Intelligence*, pages 6333–6341, 2024. 3, 7
- [45] Pengwei Yin, Guanzhong Zeng, Jingjing Wang, and Di Xie. CLIP-Gaze: Towards General Gaze Estimation via Visual-Linguistic Model. In *Proceedings of the AAAI Conference on Artificial Intelligence*, pages 6729–6737, 2024. 2, 3, 7
- [46] Ziyao Zeng, Daniel Wang, Fengyu Yang, Hyounseob Park, Stefano Soatto, Dong Lao, and Alex Wong. WorDepth: Variational Language Prior for Monocular Depth Estimation. In *2024 IEEE/CVF Conference on Computer Vision and Pattern Recognition (CVPR)*, pages 9708–9719. IEEE, 2024. 1, 3

- [47] Renrui Zhang, Ziyao Zeng, and Ziyu Guo. Can language understand depth? *Proceedings of the 30th ACM International Conference on Multimedia*, 2022. [1](#), [3](#)
- [48] Sihui Zhang, Yi Tian, Yilei Zhang, Mei Tian, and Yaping Huang. Domain-Consistent and Uncertainty-Aware Network for Generalizable Gaze Estimation. *IEEE Transactions on Multimedia*, 26:6996–7011, 2024. [7](#)
- [49] Xucong Zhang, Yusuke Sugano, Mario Fritz, and Andreas Bulling. Appearance-based gaze estimation in the wild. In *2015 IEEE/CVF Conference on Computer Vision and Pattern Recognition (CVPR)*, pages 4511–4520. IEEE, 2015. [3](#)
- [50] Xucong Zhang, Yusuke Sugano, Mario Fritz, and Andreas Bulling. Its written all over your face: Full-face appearance-based gaze estimation. In *2017 IEEE Conference on Computer Vision and Pattern Recognition Workshops (CVPRW)*, pages 2299–2308, 2017. [3](#), [4](#), [6](#)
- [51] Xucong Zhang, Yusuke Sugano, Mario Fritz, and Andreas Bulling. MPIIGaze: Real-World Dataset and Deep Appearance-Based Gaze Estimation. *IEEE Transactions on Pattern Analysis and Machine Intelligence*, 41(1):162–175, 2019. [6](#)
- [52] Xucong Zhang, Seonwook Park, Thabo Beeler, Derek Bradley, Siyu Tang, and Otmar Hilliges. ETH-XGaze: A Large Scale Dataset for Gaze Estimation Under Extreme Head Pose and Gaze Variation. *European Conference on Computer Vision*, pages 365–381, 2020. [6](#)
- [53] Wenqi Zhong, Chen Xia, Dingwen Zhang, and Junwei Han. Uncertainty Modeling for Gaze Estimation. *Transactions on Image Processing*, pages 1–1, 2024. [3](#)
- [54] Kaiyang Zhou, Jingkang Yang, Chen Change Loy, and Ziwei Liu. Learning to prompt for vision-language models. *Int. J. Comput. Vision*, 130(9):23372348, 2022. [8](#)
- [55] Ziqin Zhou, Yinjie Lei, Bowen Zhang, Lingqiao Liu, and Yifan Liu. ZegCLIP: Towards Adapting CLIP for Zero-shot Semantic Segmentation. In *2023 IEEE/CVF Conference on Computer Vision and Pattern Recognition (CVPR)*, pages 11175–11185. IEEE, 2023. [1](#), [3](#)